

The Q^2 evolution of the generalized Gerasimov-Drell-Hearn integral for the neutron using a ^3He target

M. Amarian,⁵ L. Auerbach,²⁰ T. Averett,^{6,23} J. Berthot,⁴ P. Bertin,⁴ W. Bertozzi,¹¹ T. Black,¹¹ E. Brash,¹⁶ D. Brown,¹⁰ E. Burtin,¹⁸ J.R. Calarco,¹³ G.D. Cates,^{15,22} Z. Chai,¹¹ J.-P. Chen,⁶ Seonho Choi,²⁰ E. Chudakov,⁶ E. Cisbani,⁵ C.W. de Jager,⁶ A. Deur,^{4,6,22} R. DiSalvo,⁴ S. Dieterich,¹⁷ P. Djawotho,²³ M. Finn,²³ K. Fissum,¹¹ H. Fonvieille,⁴ S. Frullani,⁵ H. Gao,¹¹ J. Gao,¹ F. Garibaldi,⁵ A. Gasparian,³ S. Gilad,¹¹ R. Gilman,^{6,17} A. Glamazdin,⁹ C. Glashauser,¹⁷ E. Goldberg,¹ J. Gomez,⁶ V. Gorbenko,⁹ J.-O. Hansen,⁶ F.W. Hersman,¹³ R. Holmes,¹⁹ G.M. Huber,¹⁶ E.W. Hughes,¹ B. Humensky,¹⁵ S. Incerti,²⁰ M. Iodice,⁵ S. Jensen,¹ X. Jiang,¹⁷ C. Jones,¹ G.M. Jones,⁸ M. Jones,²³ C. Jutier,^{4,14} A. Ketikyan,²⁴ I. Kominis,¹⁵ W. Korsch,⁸ K. Kramer,²³ K.S. Kumar,^{12,15} G. Kumbartzki,¹⁷ M. Kuss,⁶ E. Lakurigi,²⁰ G. Laveissiere,⁴ J. Leroose,⁶ M. Liang,⁶ N. Livanage,^{6,11} G. Lolos,¹⁶ S. Malov,¹⁷ J. Marroncle,¹⁸ K. McCormick,¹⁴ R. McKeown,¹ Z.-E. Meziani,²⁰ R. Michaels,⁶ J. Mitchell,⁶ Z. Papandreou,¹⁶ T. Pavlin,¹ G. Petratos,⁷ D. Pripstein,¹ D. Prout,⁷ R. Ransome,¹⁷ Y. Roblin,⁴ D. Rowntree,¹¹ M. Rvachev,¹¹ F. Sabatie,¹⁴ A. Saha,⁶ K. Slifer,²⁰ P.A. Souder,¹⁹ T. Saito,²¹ S. Strauch,¹⁷ R. Suleiman,⁷ K. Takahashi,²¹ S. Tejiro,²¹ L. Todor,¹⁴ H. Tsubota,²¹ H. Ueno,²¹ G. Urciuoli,⁵ R. Van der Meer,^{6,16} P. Vernin,¹⁸ H. Voskanian,²⁴ B. Wojtsekhowski,⁶ F. Xiong,¹¹ W. Xu,¹¹ J.-C. Yang,² B. Zhang,¹¹ P. Zolnierczuk⁸

The Jefferson Lab E94010 Collaboration

¹California Institute of Technology, Pasadena, California 91125

²Chungnam National University, Taejeon 305-764, Korea

³Hampton University, Hampton, Virginia 23668

⁴LPC IN2P3/CNRS, Université Blaise Pascal, F-63170 Aubière Cedex, France

⁵Istituto Nazionale di Fisica Nucleare, Sezione Sanità, 00161 Roma, Italy

⁶Thomas Jefferson National Accelerator Facility, Newport News, Virginia 23606

⁷Kent State University, Kent, Ohio 44242

⁸University of Kentucky, Lexington, Kentucky 40506

⁹Kharkov Institute of Physics and Technology, Kharkov 310108, Ukraine

¹⁰University of Maryland, College Park, Maryland 20742

¹¹Massachusetts Institute of Technology, Cambridge, Massachusetts 02139

¹²University of Massachusetts Amherst, Amherst, Massachusetts 01003

¹³University of New Hampshire, Durham, New Hampshire 03824

¹⁴Old Dominion University, Norfolk, Virginia 23529

¹⁵Princeton University, Princeton, New Jersey 08544

¹⁶University of Regina, Regina, SK S4S 0A2, Canada

¹⁷Rutgers, The State University of New Jersey, Piscataway, New Jersey 08855

¹⁸CEA Saclay, DAPNIA/SPhN, F-91191 Gif sur Yvette, France

¹⁹Syracuse University, Syracuse, New York 13244

²⁰Temple University, Philadelphia, Pennsylvania 19122

²¹Tohoku University, Sendai 980, Japan

²²University of Virginia, Charlottesville, Virginia 22904

²³The College of William and Mary, Williamsburg, Virginia 23187

²⁴Yerevan Physics Institute, Yerevan 375036, Armenia

We present data on the inclusive scattering of polarized electrons from a polarized ^3He target at energies from 0.862 to 5.06 GeV, obtained at a scattering angle of 15.5° . Our data include measurements from the quasielastic peak, through the resonance region, to the beginning of the deep inelastic regime, and were used to determine the virtual photon cross-section difference $\sigma_{1/2} - \sigma_{3/2}$. We extract the extended Gerasimov-Drell-Hearn integral for the neutron in the range of 4-momentum transfer squared Q^2 of 0.1–0.9 (GeV)².

Sum rules involving the spin structure of the nucleon offer an important opportunity to study Quantum Chromodynamics (QCD). At long distance scales or in the confinement regime, a sum rule of great interest is that

due to Gerasimov, Drell and Hearn (GDH) [1,2]. The GDH sum rule relates an integral over the full excitation spectrum of the spin-dependent total photoabsorption cross section to the nucleon's anomalous magnetic moment. It has not been investigated experimentally until recently [3], and further measurements are needed for a definitive test. At short distance scales or in the perturbative regime, two other sum rules, one due to Bjorken [4] and the other derived by Ellis and Jaffe [5], have provided us with significant information on nucleon spin structure through an extensive experimental and theoretical investigation [6]. These sum rules make predictions involving the first moments of the spin structure functions mea-

sured in deep inelastic scattering (DIS).

The GDH sum rule pertains strictly to the real photon case for which the four momentum transfer $Q^2=0$. DIS data, in contrast, are taken at relatively high values of Q^2 . It is desirable to have both experimental and theoretical bridges between these two very different regimes. This was achieved by generalizing the “GDH integral” to include the scattering of virtual photons for which $Q^2 > 0$ [7]. The GDH integral is often written as

$$\begin{aligned} I(Q^2) &= \int_{\nu_0}^{\infty} \frac{d\nu}{\nu} [\sigma_{1/2}(\nu, Q^2) - \sigma_{3/2}(\nu, Q^2)] \\ &= 2 \int_{\nu_0}^{\infty} \frac{d\nu}{\nu} \sigma'_{TT} \quad , \end{aligned} \quad (1)$$

where alternative generalizations are discussed in [8] and [11]. Here $\sigma_{1/2(3/2)}(\nu, Q^2)$ is the total *virtual* photoabsorption cross section for the nucleon with a projection of $\frac{1}{2}$ ($\frac{3}{2}$) for the total spin along the direction of photon momentum, ν is the electron’s energy loss, ν_0 is the pion production threshold, and σ'_{TT} is the transverse-transverse interference cross section. As $Q^2 \rightarrow 0$, $I(Q^2)$ is predicted by the original GDH sum rule:

$$I(0) = -\frac{2\pi^2\alpha}{M^2}\kappa^2, \quad (2)$$

where α is the fine structure constant, M is the mass of the nucleon, and κ is the nucleon’s anomalous magnetic moment. As $Q^2 \rightarrow \infty$, $I(Q^2) \rightarrow 16\pi^2\alpha\Gamma_1/Q^2$, where $\Gamma_1 = \int_0^1 g_1 dx$ is the first moment of the nucleon’s spin structure function g_1 , and $x = Q^2/2M\nu$ is the Bjorken scaling variable. Both Γ_1^p for the proton and Γ_1^n for the neutron have been well studied experimentally at high Q^2 [6]. At the low Q^2 limit, recent measurements have been made on $I(0)$ for the proton [3], but the neutron has yet to be measured. The two limits of the Q^2 evolution of $I(Q^2)$ are thus constrained by a combination of theory and experimental data.

It has recently been emphasized [8] that the extended GDH integral can be related [8–10] to the forward virtual Compton scattering amplitudes thus establishing a true Q^2 dependent sum rule. The original GDH sum rule and the Bjorken sum rule can both be viewed as special cases of this “extended GDH sum rule”. We note that in the Bjorken sum rule the difference of $I^p(Q^2)$ for the proton and $I^n(Q^2)$ for the neutron is considered. The extended GDH sum rule can be tested at any value of Q^2 for which the Compton amplitudes can be computed. Near $Q^2 = 0$, where the amplitudes are best understood in terms of hadronic degrees of freedom, several calculations have been performed using chiral perturbation theory (χ PT) [8,12,10,13]. The two most recent of these efforts, which take different approaches, include next-to-leading order corrections [12,13]. An important issue is the highest values of Q^2 at which the calculations are valid, with estimates ranging as high as 0.3 GeV^2 [13].

For large Q^2 , a region best described by partonic degrees of freedom, Operator Product Expansion (OPE) techniques have been used to express the Compton amplitudes as a perturbative series in α_s and a (higher twist) power series in $1/Q^2$. The predictions of the Bjorken sum rule can thus be extended to finite Q^2 , perhaps as low as $Q^2 \sim 0.5 \text{ GeV}^2$ [12]. For lower values of Q^2 , that are still well above the range where χ PT is applicable, there is currently little theoretical guidance. This transition region, however, is well suited to the use of lattice QCD [15]. Mapping out $I(Q^2)$ experimentally, as we have done in this paper for the range of $0.1 \text{ GeV}^2 \leq Q^2 \leq 0.9 \text{ GeV}^2$, is an important step to testing these ideas and building our understanding of the dynamics of nonperturbative QCD.

We measured the inclusive scattering of longitudinally polarized electrons from a polarized ^3He target in Hall A of the Thomas Jefferson National Accelerator Facility (JLab). Data were collected at six incident beam energies: 5.06, 4.24, 3.38, 2.58, 1.72, and 0.86 GeV, all at a nominal scattering angle of 15.5° . The measurements covered values of the invariant mass W from the quasielastic peak (not discussed in this paper), through the resonance region, to the values indicated in Fig. 1. Data were taken for both longitudinal and transverse target polarization orientations. Both spin asymmetries and absolute cross sections were measured.

A cw beam of polarized electrons was produced by illuminating a strained GaAs photocathode with circularly polarized light. Beam currents were limited to $10\text{--}15 \mu\text{A}$ to minimize depolarization of the target. The average polarization of the electron beam was 0.70 ± 0.03 , and was monitored using a double arm Møller polarimeter. The polarization was typically reversed at a rate of 1 Hz.

The ^3He target was polarized by spin-exchange with optically pumped rubidium (Rb) [16]. Built specifically for this and subsequent experiments in Hall A, the design of the target is similar to that built at SLAC for E142 [17], but with greater flexibility for polarization direction and increased capacity for handling higher average beam currents [18,19]. The average in-beam polarization was 0.35 ± 0.014 . The ^3He gas was contained in sealed glass cells with densities corresponding to $10\text{--}12 \text{ atm}$ at 0°C . A small quantity (about 70 Torr) of nitrogen was also present to aid in the optical pumping process. The portion of the cell in the electron beam, the target chamber, was a long cylinder approximately 40 cm in length. The length was chosen so that the glass end windows of the cell were at the edge of the acceptance of the spectrometers. The portion of the cell in which optical pumping took place, the pumping chamber, was irradiated with about 90 W of light from high-power diode-laser arrays with their wavelength centered at the first transition line of Rb (795 nm). The polarization of the ^3He was monitored by the NMR technique of adiabatic fast passage (AFP) [20]. The response of the NMR system was cal-

ibrated by two methods. In one method the AFP signals of ^3He were compared with the AFP signals from water which had a small polarization due to the usual Boltzmann distribution. In the other method AFP signals were observed following a determination of the ^3He polarization using a shift of the Rb EPR lines due to collisions with polarized ^3He atoms [21]. Independent verification of our target polarimetry at the level of 4% was provided by measuring the asymmetry in elastic scattering [22,23], which depends on the product of the target and beam polarizations.

The scattered electrons were detected using the two Hall A high resolution spectrometers. Momenta were determined by track analysis, and particle identification was accomplished using gas Cerenkov detectors and lead-glass shower counters. Pion rejection was better than 10^3 in both spectrometer arms, which was more than sufficient since the π/e ratio was never worse than 10.

The quantities we measure experimentally are related to σ'_{TT} and the transverse-longitudinal interference term σ'_{LT} in the Born approximation according to the relations

$$\frac{d^2\sigma^{\downarrow\uparrow}}{d\Omega dE'} - \frac{d^2\sigma^{\uparrow\uparrow}}{d\Omega dE'} = B(\sigma'_{TT} + \eta\sigma'_{LT}) \quad (3)$$

and

$$\frac{d^2\sigma^{\downarrow\Rightarrow}}{d\Omega dE'} - \frac{d^2\sigma^{\uparrow\Rightarrow}}{d\Omega dE'} = B\sqrt{\frac{2\epsilon}{1+\epsilon}}(\sigma'_{LT} - \zeta\sigma'_{TT}) \quad (4)$$

where $d^2\sigma^{\downarrow\uparrow(\uparrow\uparrow)}/d\Omega dE'$ is the cross section for the case in which the beam and target spin directions are antiparallel (parallel), and the left side of (4) represents the corresponding quantity for transverse target spin orientation. Also $B = 2(\alpha/4\pi^2)(K/Q^2)(E'/E)(2/(1-\epsilon))(1-E'\epsilon/E)$, where E and E' are the initial and final electron energies, $\epsilon^{-1} = 1 + 2[1 + Q^2/4M^2x^2]\tan^2(\theta/2)$, θ is the scattering angle in the laboratory frame, $\eta = \epsilon\sqrt{Q^2}/(E - E'\epsilon)$, and $\zeta = \eta(1 + \epsilon)/2\epsilon$. The factor K represents the virtual photon flux and is convention dependent. We use the convention $K = \nu - Q^2/2M$, due to Hand [24].

To extract from our raw ^3He data σ'_{TT} , which is defined within the Born approximation, we must first apply ‘‘radiative corrections’’ to account for the emission of real and virtual photons. These corrections were performed using the procedure first described by Mo and Tsai for the case of unpolarized scattering [25], and extended to include polarized effects using the program POLRAD [26]. For our experiment, we incorporated into POLRAD our actual data for the quasielastic and resonance regions, as their effect on the radiative corrections are significant. The results for σ'_{TT} are shown in Fig. 1 as a function of the invariant mass W for each of the six energies measured, and represent the neutron to the extent that we have set M equal to the neutron mass in equations (3) and (4). We note, though, that for σ'_{TT} , no corrections

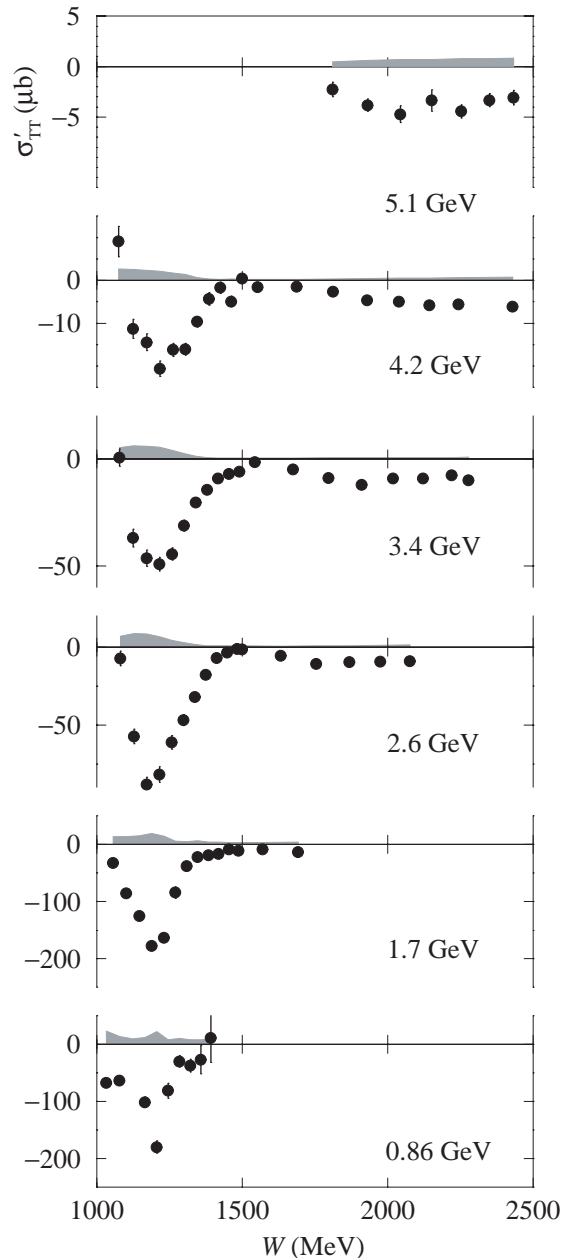


FIG. 1. σ'_{TT} is plotted as a function of invariant mass W for each of the six incident energies studied.

for nuclear effects were applied. The error bars are due to statistics only, with the grey bands indicating systematic errors. The error due to radiative corrections, which dominates the systematic errors on σ'_{TT} , was taken as 20% of the applied correction for all but the lowest energy where 40% was assumed. Other systematic errors included a relative uncertainty in normalization of 5% from absolute cross section, 4% from target polarization, and 4% from beam polarization.

To compute $I(Q^2)$, σ'_{TT} is needed at constant Q^2 . We chose six equally spaced values of Q^2 in the range $0.10 \text{ GeV}^2 \leq Q^2 \leq 0.9 \text{ GeV}^2$ and determined σ'_{TT} from

our measured points by interpolation, or for a few points, extrapolation. The results are plotted in Fig. 2 as a function of ν . The prominent peak in the cross section is the

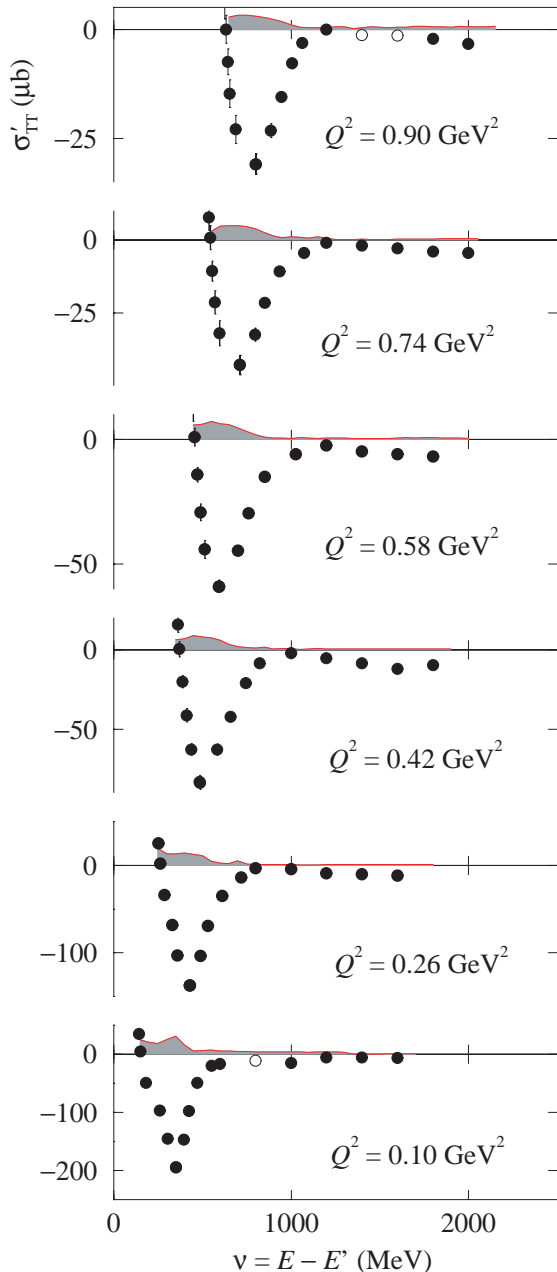


FIG. 2. σ'_{TT} is plotted as a function of energy loss ν for each of six values of constant Q^2 . The points shown with solid (open) circles were determined by interpolation (extrapolation).

Δ_{1232} resonance, which decreases in magnitude with increasing Q^2 . The error bars represent the uncertainty due to statistics, and the grey bands indicate the uncertainty due to systematic errors, which in addition to those shown in Fig. 1, include a contribution from interpolation and extrapolation.

The extended GDH integral was computed for each

value of Q^2 according to eq. 1 using limits of integration extending from the nucleon pion threshold to a value of ν corresponding to $W = 2.0$ GeV. The results are given in Table I. Before plotting our results, we have applied a correction to account for the fact that our neutron is embedded in a ^3He nucleus using a calculation due to Ciofi degli Atti and Scopetta [27]. This procedure introduces an additional 5% systematic uncertainty in our result. Our results for $I(Q^2)$ for the neutron, with the integration covering roughly the resonance region, are shown in Fig. 3 using open circles. The error bars, when visible, represent statistical uncertainties only, and the systematic effects are shown with the grey band. We have made an estimate of the unmeasured strength in $I(Q^2)$ for the region $4 \text{ GeV}^2 < W^2 < 1000 \text{ GeV}^2$ using the parameterization of Thomas and Bianchi [29] (1000 GeV^2 was the highest value considered in their paper). The solid squares have this estimate included, and an estimate of the theoretical uncertainty has already been included in the systematic error shown.

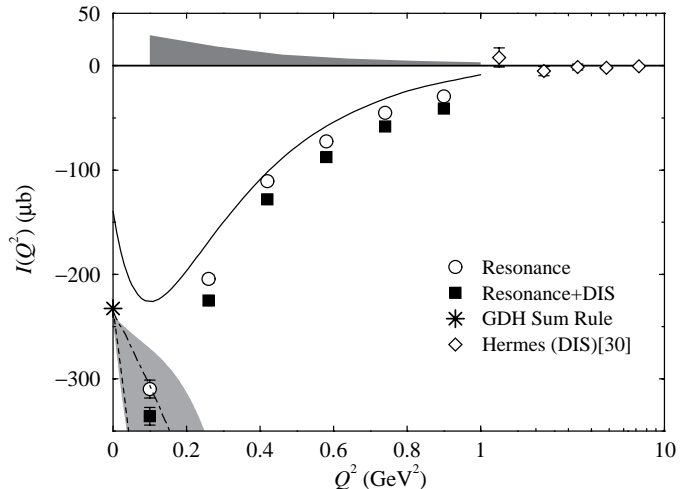


FIG. 3. Our measurements for $I(Q^2)$ vs. Q^2 , both with and without an estimate of the DIS contribution. Also shown with a dotted (dot-dashed) line are the χ PT calculations of ref. [12] (refs. [13] and [14]). The calculation of ref. [11], based largely on the MAID model, is shown with a solid line. We have included data from HERMES [30], and to avoid compressing our horizontal scale, we have adopted a semi-log scale for $1 \text{ GeV}^2 < Q^2$.

| Q^2 (GeV 2) | I_{GDH} (μb) | Statistical (μb) | Systematic (μb) |
|-------------------|------------------------------------|-------------------------------|------------------------------|
| 0.10 | -223.76 | 6.18 | 23.68 |
| 0.26 | -156.52 | 3.01 | 13.58 |
| 0.42 | -88.73 | 2.10 | 7.46 |
| 0.58 | -59.56 | 1.51 | 4.56 |
| 0.74 | -37.96 | 1.43 | 3.14 |
| 0.90 | -23.63 | 1.00 | 2.09 |

TABLE I. Measured values for $I(Q^2)$ prior to nuclear corrections together with statistical and systematic errors.

Our data indicate a smooth variation of $I(Q^2)$ to increasingly negative values as Q^2 varies from 0.9 GeV^2 toward zero. Our data are more negative than the prediction of Drechsel, Kamalov, and Tiator, whose calculation is mostly based on the phenomenological model MAID, and is shown on Fig. 3 as a solid line [11]. Their prediction includes contributions to $I(Q^2)$ for $W \leq 2 \text{ GeV}$, and should thus be compared with the open circles. At high Q^2 , our data approach those of HERMES, which spans the range $1.28 \text{ GeV}^2 < Q^2 < 7.25 \text{ GeV}^2$ [30], but includes only the DIS part of the GDH integral. It is desirable to compare our data with the GDH sum rule prediction $I(0) = -232.8 \mu b$. This prediction is indicated on Fig. 3, along with extensions to $Q^2 > 0$ using two χ PT calculations, that described in [12] (dotted line) and collectively in [13] and [14] (dot-dashed line). Taken together, [13] and [14] describe an extended calculation including resonance effects, and have associated with them a large error (shown with a grey band) due to the uncertainty in certain resonance parameters. The error can be seen to encompass both our lowest Q^2 point and the calculation of [12]. We note, though, that at $Q^2 = 0.3 \text{ GeV}^2$, the prediction of [13] and [14] is much more negative than our data. We look forward to both further calculations as well as further measurements [31].

In conclusion we have made the first measurements of σ'_{TT} and the generalized GDH integral $I(Q^2)$ of the neutron at low Q^2 ($0.1 \text{ GeV}^2 \leq Q^2 \leq 0.9 \text{ GeV}^2$). The data show a dramatic change in the value of the integral from what is observed at high Q^2 ($0.9 \text{ GeV}^2 < Q^2$). While not unexpected from phenomenological models, our data illustrate the sensitivity of $I(Q^2)$ to the transition from partonic to hadronic behavior. Our data provide a precision data base for twist expansion analysis, provide a check of χ PT calculations, and establish an important benchmark against which one can compare future calculations and measurements of low Q^2 spin structure.

We would like to thankfully acknowledge the untiring support of the JLab staff and accelerator division. This work was supported by the U.S. Department of Energy (DOE), the DOE-EPSCoR, the U.S. National Science Foundation, NSERC of Canada, the European INTAS Foundation, the Italian INFN, and the French CEA, CNRS, and Conseil Régional d'Auvergne. The South-eastern Universities Research Association (SURA) operates the Thomas Jefferson National Accelerator Facility for the DOE under contract DE-AC05-84ER40150.

[1] S. B. Gerasimov, Sov. J. of Nucl. Phys. **2**, 430 (1966).

[2] S. D. Drell, and A. C. Hearn, Phys. Rev. Lett. **16**, 908 (1966).

- [3] J. Ahrens *et al.* (The GDH and A2 Collaborations), Phys. Rev. Lett. **87**, 022003-1 (2001).
- [4] J. D. Bjorken, Phys. Rev. **148**, 1467 (1966); Phys. Rev. D **1**, 465 (1970); Phys. Rev. D **1**, 1376 (1970).
- [5] J. Ellis and R. L. Jaffe, Phys. Rev. D **9**, 1444 (1974); Phys. Rev. D **10**, 1669 (1974).
- [6] For recent reviews, see E. W. Hughes and R. Voss, Ann. Rev. Nucl. Part. Sci **49**, 303 (1999) or B. W. Filippone and X. Ji, hep-ph/0101224v1, and references therein.
- [7] M. Anselmino, B. L. Ioffe, and E. Leader, Sov. J. Nucl. Phys. **49**, 136 (1989).
- [8] X. Ji and J. Osborne, J. Phys. G **27**, 127 (2001).
- [9] B.L. Ioffe, **Hard Processes** Vol. 1, North-Holland (1984).
- [10] V. Bernard, N. Kaiser, and Ulf-G. Meißner, Phys. Rev. D **48**, 3062 (1993); Int. J. Mod. Phys. **E4**, 193 (1995).
- [11] D. Drechsel, S.S. Kamalov, and L. Tiator, Phys. Rev. D **63**, 114010 (2001). Note, model I_C is plotted in Fig. 3.
- [12] X. Ji, C. Kao, and J. Osborne, Phys. Lett. **B 472**, 1 (2000).
- [13] V. Bernard, T.R. Hemmert, and Ulf-G. Meißner, hep-ph/0203167.
- [14] V. Bernard and Ulf-G. Meißner, private communication.
- [15] Nathan Isgur, John W. Negele, *et al.*, *Nuclear Theory with Lattice QCD*, a proposal submitted to the U.S. Department of Energy, *unpublished* (2000).
- [16] See for instance T. G. Walker and W. Happer, Rev. Mod. Phys. **69**, 629 (1997), and references therein.
- [17] P. L. Anthony *et al.* (the SLAC E-142 collaboration), Phys. Rev. Lett. **71**, 959 (1993); Phys. Rev. D **54**, 6620 (1996).
- [18] J.S. Jensen, Ph.D. Thesis, California Institute of Technology, 2000 (unpublished); I. Kominis, Ph.D. Thesis, Princeton University, 2000 (unpublished).
- [19] Details of JLab E94-010 and relevant theses can be found at www.jlab.org/e94010/.
- [20] A. Abragam, *Principles of Magnetic Resonance*, Oxford University Press, Oxford (1961).
- [21] M.V. Romalis and G.D. Cates, Phys. Rev. A **58**, 3004 (1998).
- [22] A. Deur, Ph.D. Thesis, Université Blaise Pascal, (Ref. # PCCFT0003) 2000 (unpublished).
- [23] W. Xu *et al.* (the JLab E95-001 collaboration), Phys. Rev. Lett. **85**, 2900 (2000).
- [24] L.N. Hand, Phys. Rev. **129**, 1834 (1963).
- [25] L.W. Mo and Y.S. Tsai, Rev. Mod. Phys. **41**, 205 (1969); Y.S. Tsai, Report No. SLAC-PUB-848 (1971).
- [26] I.V. Akushevich and N.M. Shumeiko, J. Phys. **G 20**, 513 (1994).
- [27] C. Ciofi degli Atti and S. Scopetta, Phys. Lett. **B 404**, 223 (1997).
- [28] F.J. Gilman, Phys. Rev. **167**, 1365 (1968).
- [29] E. Thomas and N. Bianchi, Nucl. Phys. **B 82** (Proc. Suppl.), 256 (2000).
- [30] K. Ackerstaff *et al.* (The HERMES Collaboration), Phys. Lett. **B 444**, 531 (1998).
- [31] See for example Jefferson Laboratory Proposal E97-110, J.-P. Chen, A. Deur, and F. Garibaldi spokespersons.